

ULF Wave Indices to Characterize the Solar Wind–Magnetosphere Interaction and Relativistic Electron Dynamics

Natalia ROMANOVA^{1,2} and Viacheslav PILIPENKO³

¹Institute of the Physics of the Earth, Moscow, Russia
e-mail: runatka@mail.ru

²Belgian Institute for Space Aeronomy, Brussels, Belgium

³Space Research Institute, Russian Academy of Sciences, Moscow, Russia
e-mail: pilipenko_va@mail.ru

Abstract

To quantify the level of low-frequency wave activity of the magnetosphere and IMF, a set of the ULF wave power indices has been introduced. We demonstrate that the ULF activity global level can be very useful in space weather related problems. The application of the interplanetary index to an analysis of auroral activity driving has shown that a turbulent IMF drives auroral activity more strongly than the laminar solar wind does. The enhancements of relativistic electrons at the geosynchronous orbit are known not to be directly related to the intensity of magnetic storms. We found that the electron dynamics correlated well with long-lasting intervals of elevated ground ULF wave index. This fact confirms the importance of magnetospheric ULF turbulence in energizing electrons up to relativistic energies. The time-integrated ULF index demonstrates a significantly higher correlation with electron fluxes, which implies the occurrence of a cumulative effect in the electron energization.

Key words: ULF waves, MHD turbulence, solar wind–magnetosphere interaction, electron acceleration.

1. INTRODUCTION

The interaction between the solar wind (SW) and terrestrial magnetosphere is the primary driver of many processes and phenomena occurring in the magnetosphere. This interaction has often been viewed using the implicit assumption of quasi-steady and laminar plasma flow. However, many of the energy transfer processes in the magnetospheric boundary regions have a sporadic/bursty character, and observations have highlighted the importance of including the effects of turbulence as well (Antonova 2000, Borovsky and Funsten 2003). Ultra-low frequency (ULF) waves in the Pc5 (2-7 mHz) band are a ubiquitous aspect of the SW interaction with the Earth's magnetosphere. The turbulent character of SW drivers and the existence of natural MHD waveguides and resonators in near-terrestrial space in the lower ULF frequency range (1-10 mHz) ensures a quasi-periodic magnetic field response to forcing at the boundary layers. Therefore, much of the turbulent nature of plasma processes of SW–magnetosphere interactions can be monitored with ground or space observations in the ULF range.

Progress in understanding and monitoring the turbulent processes in space physics is hampered by the lack of convenient tools for their characterization. Various geomagnetic indices (Kp , Dst , AE , PC , etc.) quantify the energy supply in certain regions of the coupled SW-magnetosphere-ionosphere system, and are used as primary tools in statistical studies of solar-terrestrial relationships. However, these indices characterize the steady-state level of the electrodynamics of the near-Earth environment. Until recently there was no index characterizing the turbulent character of the energy transfer from the SW into the upper atmosphere and the short-scale variability of near-Earth electromagnetic processes. A new hourly ULF index using the spectral ULF power in frequency band from 1-2 mHz to 8-10 mHz has been introduced by Kozyreva *et al.* (2007). This wave power index characterizes the ground ULF wave activity on a global scale and is calculated from a world-wide magnetometer array. The ground power index is augmented by interplanetary and geostationary ULF wave indices, as indicators of the turbulent state of the interplanetary space and magnetosphere.

In this paper we validate the significance of these ULF indices for statistical studies of various aspects of solar-terrestrial relationships and demonstrate their merits and disadvantages.

2. THE ALGORITHM OF THE ULF WAVE INDEX CONSTRUCTION

Algorithm of the ULF wave index (Kozyreva *et al.* 2007) relies on the estimate of the ULF wave power $F_j = B_j^2(f)$ in the band Δf from f_L to f_H averaged over N_c components ($j = 1, 2, \dots, N_c$):

$$ULF = \frac{1}{N_c} \left[\Delta f \sum_j \int_{f_l}^{f_h} F_j(f) df \right]^{1/2}.$$

The signal component S of the spectral power is calculated in a similar way, but with the background spectral power $F^{(B)}(f)$ subtracted from the total spectral power $F(f)$, namely $F_j(f) \rightarrow F_j(f) - F_j^{(B)}(f)$. The background spectrum is determined as a least-square fit of the power-law spectral form $F^{(B)}(f) \propto f^{-\alpha}$ in a chosen frequency band. The spectral power below $F^{(B)}(f)$ is attributed to noise $N_j(f)$, so $T_j = S_j + N_j$. The final product is composed from the set of hourly ULF wave indices:

□ **Ground ULF wave index** (T_{GR}, S_{GR}) is a proxy of global ULF activity. For its production, the algorithm selects the peak value of wave powers of two horizontal components from all the 1-min magnetic stations in the sector from 05 to 15 MLT (to avoid irregular nighttime disturbances), and in the latitudinal range from 60° to 70° geomagnetic latitudes.

However, ground magnetic fluctuations are not always a perfect image of the ULF fluctuations in the magnetosphere. For example, there is a class of ULF waves, called storm-related Pc5 pulsations that occur during the recovery phase of magnetic storms. These ULF waves are generated by ring current protons *via* various kinds of drift instabilities (Pilipenko 1990). Despite their high amplitudes in the magnetosphere, these pulsations are rarely if ever seen on the ground because of their small azimuthal scales and subsequent screening by the ionosphere. Thus, the ground global index has been augmented by a similar index, estimated from data from space magnetometers.

□ **Geostationary ULF wave index** (T_{GEO}, S_{GEO}) is calculated from 1-min 3-component magnetic data from GOES satellites to quantify magnetic fluctuations in the region of geostationary orbit.

□ **Interplanetary ULF wave index** (T_{IMF}, S_{IMF}) to quantify the short-term IMF variability is calculated from the time-shifted 1-min data from one of the available interplanetary satellites, such as WIND, ACE, IMP-8, or 1-min OMNI database.

Further we demonstrate that a wide range of space physics studies benefits from the introduction of the ULF wave index. In our study we have used only the narrow-band ULF S indices, though the results obtained with wide-band indices T have turned out to be nearly the same.

3. ULF WAVE INDEX AS AN IMPORTANT SPACE WEATHER PARAMETER

The turbulent/eddy viscosity of the SW flow passing the magnetosphere is controlled to a considerable extent by the level of upstream turbulence.

However, the turbulence level of the magnetosheath plasma, which directly interacts with the magnetosphere, can differ significantly for different IMF orientations in respect to the bow shock (Shevyrev and Zastenker 2005). Nonetheless, the degree of coupling of the SW flow to the magnetosphere appears to be influenced by the level of SW/IMF turbulence upstream of the Earth. The eddy (turbulent) viscosity concept predicts that the coupling will be lessened when the level of upstream turbulence is lessened. The effective Reynolds numbers of the SW and magnetosheath flows and that of the internal magnetospheric flows are very high, so the magnetosphere behaves as a turbulent high-Reynolds-number system. Therefore, the presence of turbulence inside and outside the magnetosphere should have profound effects on the large-scale dynamics of the system through eddy viscosity and diffusion.

Using the introduced ULF index of the IMF variability, here we verify the fact that when the SW is more turbulent, the effective degree of its coupling to magnetosphere is higher. Figure 1 shows the histogram of the occurrence probability of $\log S_{IMF}$ index. The IMF may be considered as noisy when $\log S_{IMF} > 0$, and IMF is calm when $\log S_{IMF} < 0$.

Auroral response, as characterized by hourly AE index, is compared in Fig. 2 with a strength of the SW driver, determined by the IMF B_z component, for the laminar (right-hand panel) and turbulent (left-hand panel) IMF for the period 1994-1995. Comparison of median curves shows that under southward IMF ($B_z < 0$), AE grows nearly linearly upon increase of the magnitude of B_z , whereas the average AE response to the turbulent IMF is higher. This difference is significant not only for northward IMF, when one expects the viscous interaction to be dominant over the reconnection, but it reveals itself even under southward IMF. This comparison confirms that the magnetosphere is driven more strongly when the IMF turbulence level is elevated.

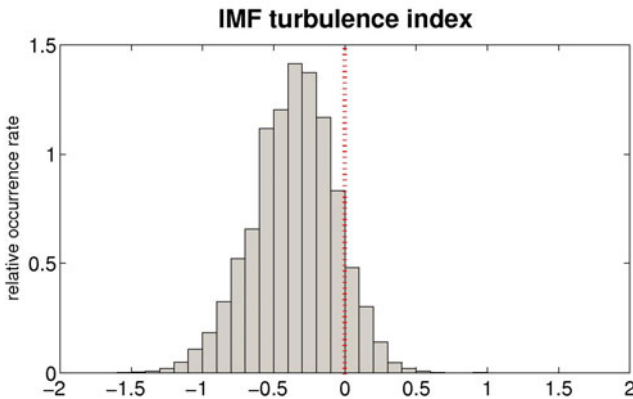


Fig. 1. The occurrence probability of the $\log S_{IMF}$ index. The vertical dotted line denotes a chosen boundary between the quiet and turbulent IMF.

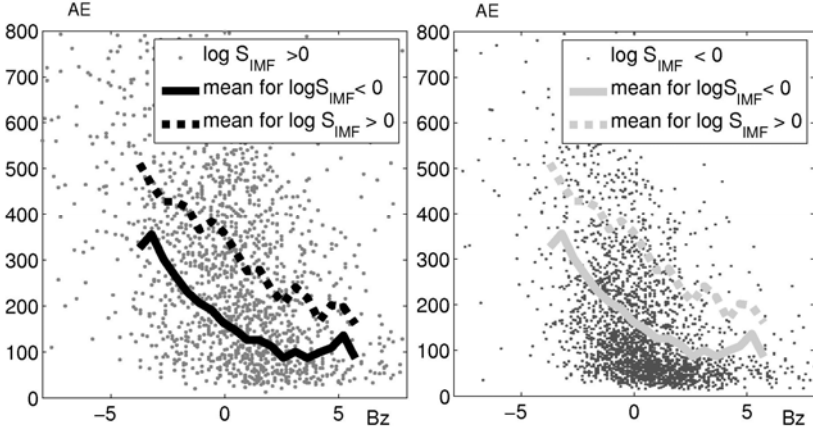


Fig. 2. The dependence of auroral activity (AE index) on the IMF driver (Bz) for laminar, $\log(S_{IMF}) < 0$, and turbulent, $\log(S_{IMF}) > 0$, IMF.

The availability of an interplanetary ULF index gives us a possibility to visualize the relationship between the SW/IMF turbulence and interplanetary parameters. We have analyzed hourly values of IMF, SW, and the interplanetary ULF index. To reveal the significance of the IMF orientation on the interplanetary fluctuations we have divided all values into northward IMF events, when $Bz > 0$, and southward IMF events, when $Bz < 0$.

The correspondence between the interplanetary ULF index S_{IMF} and the SW velocity V (Fig. 3, left-hand panel) has the following features. The power of IMF fluctuations grows with increase of the SW velocity in a similar way under northward (blue dots) and southward (red dots) IMF orientation. However, this growth becomes slower with the increase of the SW velocity (compare with the linear fit shown by a dashed line). The statistical “swarm” of scatter samples has a clear low cut-off boundary, which means that for a particular V the intensity of IMF fluctuations cannot be less than a certain value. This low boundary of possible ULF fluctuation intensity grows with increase of V . On the other hand, there is also an upper cut-off, which is V -independent, indicating that for any SW velocity the IMF fluctuations cannot exceed some saturation level. The occurrence of cut-off lower and upper boundaries signifies that the intensity of IMF fluctuations is within certain limits for any V .

Is the SW velocity the only controlling factor of IMF wave turbulence, or may the IMF orientation be of some importance for ULF variability too? To answer this question we analyze the distributions of S_{IMF} index for positive and negative Bz values (Fig. 3, right-hand panel). The distribution has turned out to be symmetric, so the level of IMF fluctuations does not depend on IMF north-south orientation.

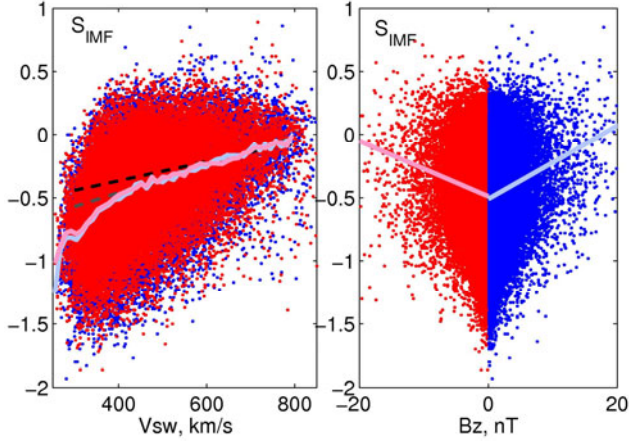


Fig. 3. Correspondence between the interplanetary ULF magnetic fluctuations, as characterized by $\log(S_{IMF})$ index, and (left-hand panel) SW velocity V for IMF $B_z > 0$ (blue dots) and $B_z < 0$ (red dots), and (right-hand panel) IMF orientation B_z . The light blue and magenta lines denote the running mean for positive and negative IMF B_z events, correspondingly. For an eye guidance the linear fit is shown by dashed line.

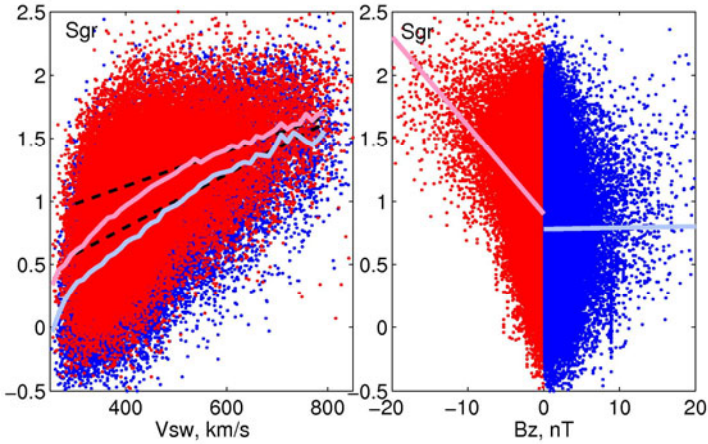


Fig. 4. Correspondence between the global ground ULF activity, as characterized by $\log(S_{GR})$, and the SW velocity V (left-hand panel) for IMF $B_z > 0$ (blue dots) and $B_z < 0$ (red dots). The right-hand panel shows the $\log(S_{GR})$ dependence on the IMF orientation. The running mean for negative and positive IMF B_z are denoted by magenta and light blue lines.

Numerous studies showed that the key parameter that controls the ground ULF activity is the SW velocity (e.g., Engebretson *et al.* 1998). The correspondence between the hourly values of ground ULF index S_{GR} and V

(Fig. 4, left-hand panel) confirms this result. The scatter plot shows that the ground ULF wave power grows with increase of V . This growth becomes less steep for high speed SW, as evident from the running mean lines for both negative (magenta) and positive (light blue) IMF B_z . The statistical swarm of scatter points has a clear cut-off lower boundary and an upper cut-off, similar to the IMF turbulence, indicating that for any V the ground wave activity cannot exceed some saturation level. The occurrence of cut-off lower and upper boundaries signifies that the intensity of ground fluctuations can be within certain limits only for any V . These statistical features should be understood in the framework of the theory of ULF wave excitation through the SW shear flow instability.

In order to check whether the SW velocity is the only controlling factor of magnetospheric wave activity, we have separated all data samples into positive IMF events ($B_z > 0$) and negative events ($B_z < 0$). Figure 4 (left-hand panel) shows that northward (blue dots) and southward (red dots) events have the same dependence on V , but, in contrast to the interplanetary fluctuations, under southward IMF the ground ULF wave activity is higher. The distribution of S_{GR} and B_z samples (Fig. 4, right-hand panel) is also skewed: for $B_z < 0$ the ground wave power is generally higher than for $B_z > 0$. Thus, the reconnection and particle injection processes, both controlled by B_z , contribute to the generation of magnetospheric ULF activity.

The availability of the ULF wave indices enables one not only to visualize possible interconnections between ULF turbulence and various solar weather parameters, but to perform easily a more rigorous statistical analysis. As an example, the results of the cross-correlation analysis of ground

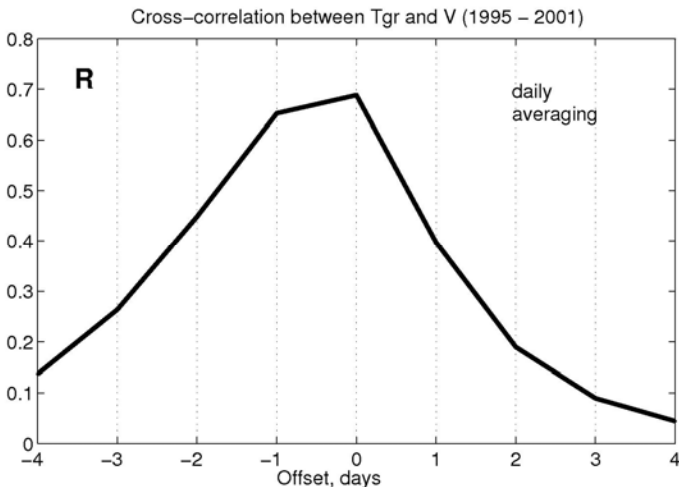


Fig. 5. The coefficient of cross-correlation between hourly values of $\log(T_{GR})$ and V .

ULF activity, as characterized by S_{GR} index, and the SW velocity are given in Fig. 5. The asymmetry of the cross-correlation function indicates that the increase of magnetospheric ULF activity starts statistically earlier than the increase of V . This may signify that the shear flow instability is not the only mechanism of ULF wave generation, but the irregular SW plasma density enhancements preceding the occurrence of high-speed streams contribute also into ULF wave excitation. Such observations were also reported by Kleimenova *et al.* (2003), and Engebretson *et al.* (1998), who also presented a simple model to explain the geoeffectiveness of such enhancements. Indeed, the SW V and N show a strong statistical anti-correlation with a shifted peak of cross-correlation function by about 0.5 day (not shown) indicating that variations of N precede those of V .

4. ULF WAVE INDEX AND “KILLER” ELECTRONS

Here we consider application of the ULF wave index to the problem of magnetospheric electron acceleration up to relativistic energies. The relativistic electron events are not merely a curiosity for scientists, but they can have disruptive consequences for spacecraft (Pilipenko *et al.* 2006).

Commonly, relativistic electron enhancements in the outer radiation belt are associated with magnetic storms (Reeves 1998), though the wide variability of the response and the puzzling time delay of ~ 2 days between storm main phase and the response has frustrated the identification of responsible mechanisms. Moreover, some electron events may occur even without magnetic storm or during very mild storms ($|Dst| \sim 0-40$ nT). An example of such an event in December 1999 is shown in Fig. 6. In this situation a high-speed solar stream occurs without a favorable B_z , and consequently without a noticeable storm (as measured by the Dst index).

The efficiency of these non-identified mechanisms of the energetic electron acceleration is strongly enhanced upon an increase of V . Because the SW does not interact directly with magnetospheric electrons, some intermediary must more directly provide energy to the electrons. Rather surprisingly, ULF waves in the Pc5 band (\sim few mHz) have emerged as a possible energy reservoir (Rostoker *et al.* 1998): the presence of Pc5 wave power after minimum of Dst was found to be a good indicator of relativistic electron response (O'Brien *et al.* 2001). Therefore, in a laminar, non-turbulent magnetosphere the “killer” electrons would not appear. The mechanism of the acceleration of ~ 100 keV electrons supplied by substorms is a revival of the idea of the magnetospheric geosynchrotron: pumping of energy into seed electrons is provided by large-scale MHD waves in a resonant way, when the wave period matches the multiple of the electron drift period (Elkington *et al.*

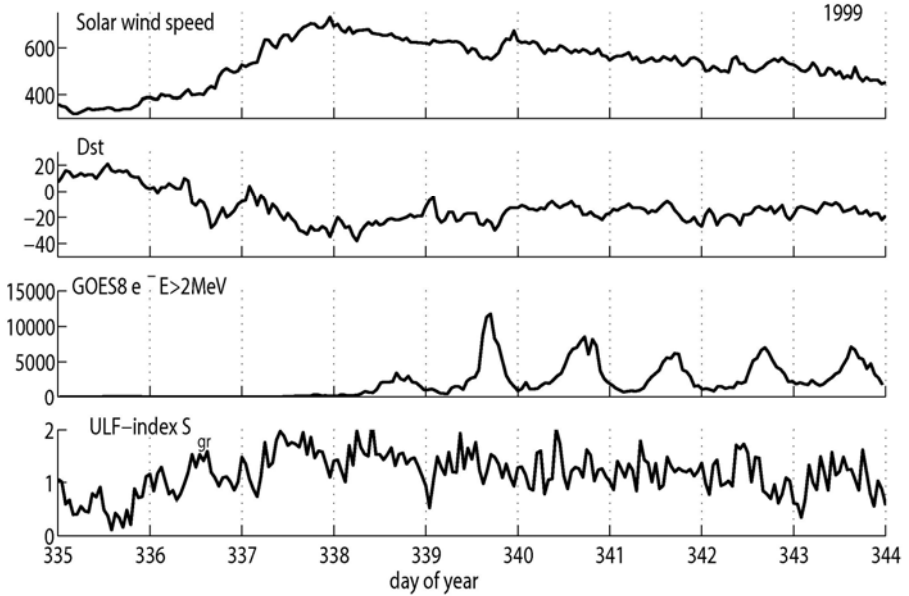


Fig. 6. The “electron event” without magnetic storm observed at GOES-8 during December 1999.

1999, Ukhorskiy *et al.* 2005). However, this mechanism is not the only one. Local resonant acceleration upon interaction with high-frequency chorus emissions was claimed to be responsible for the relativistic electron occurrence (Meredith *et al.* 2003).

A long-term persistent ULF activity can be more important for electron acceleration than short-term, though intense, ULF bursts. Thus, the cumulative ULF index:

$$\langle S_{GR}(t) \rangle = \int_{-\infty}^t S_{GR}(t') \exp\left[-\frac{(t-t')}{\tau}\right] dt'$$

integrated over time pre-history τ might be a better parameter than the instant ULF index. Visual comparison between the *Dst* index, electron fluxes at geostationary orbit, and both instant and cumulative ULF indices (S_{GR} and $\langle S_{GR} \rangle$ with $\tau = 4$ days) during a selected period in 1994 is shown in Fig. 7. This plot illustrates that any magnetic storm is accompanied by the GEO relativistic electron enhancement, as highlighted by dashed arrows. However, there is no simple correspondence between the magnetic storm intensity and magnitude of electron enhancement. The bottom panel of Fig. 7 prompts that the ULF index, and especially the integrated ULF index, characterizes the electron dynamics much better than *Dst* index.

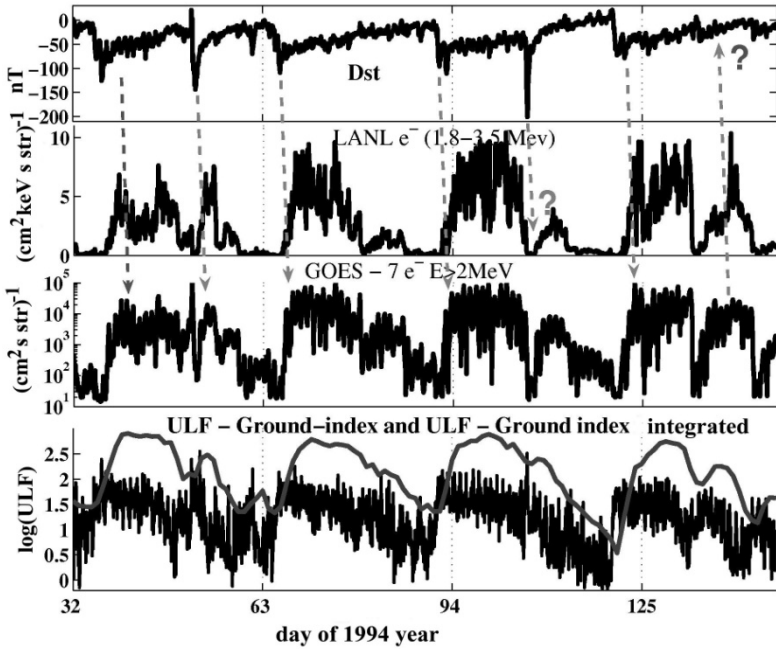


Fig. 7. Comparison between the Dst index, electron fluxes at geostationary orbit measured by LANL J_e ($\text{cm}^2 \text{keV s str}^{-1}$) and GOES-7 J_e ($\text{cm}^2 \text{s str}^{-1}$), cumulative index $\log\langle S_{GR} \rangle$ (solid line, bottom panel), and ULF index $\log(S_{GR})$ during days 32-150 of 1994.

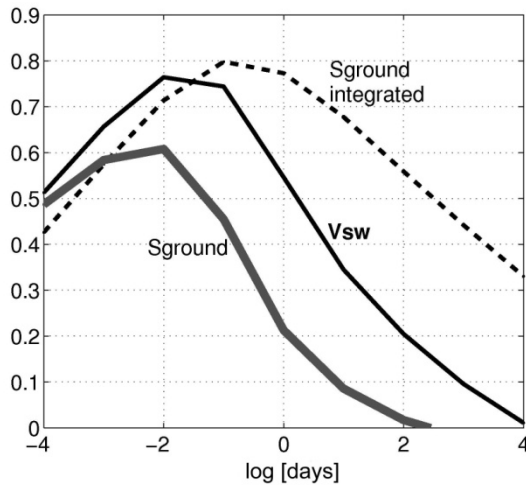


Fig. 8. The cross-correlation function between the hourly values of the electron flux at geostationary orbit measured by LANL, and the SW velocity (thin line), cumulative ULF index $\log\langle S_{GR} \rangle$ (dashed line), and ULF index $\log(S_{GR})$ (thick line).

Indeed, the correlation of electron flux with the integrated ULF index, estimated for the period 1992-1996, increases substantially, from 0.5 to 0.8 (Fig. 8), and even becomes slightly higher than the correlation with the SW velocity. The cross-correlation function shows that the elevated level of ULF wave activity precedes the peak of relativistic electron flux for about 2-4 days, whereas the same delay for the cumulative index is about 1 day. This increase of correlation probably implies the occurrence of a cumulative effect of some diffusion process. Thus, the long-lasting ULF wave activity is more important for the electron acceleration than just instant bursts of wave activity.

5. DISCUSSION AND CONCLUSIONS

The solar wind supplies energy to the magnetosphere, at the rate of $\sim 10^{10}$ to 10^{12} J/s, in order to account for energy dissipated in the auroral oval and required for ring current formation. Most of the time we cannot interpret our observations in terms of steady-state magnetospheric models. Any steady-state assumptions are in fact invalid because the solar wind represents a rapidly time-varying environment to which the magnetosphere is continuously exposed, for example, the IMF B_z component fluctuates on a characteristic time scale far shorter than the impulse response time of the magnetosphere. The space community has been recently provided with a new convenient tool for the characterization and monitoring of the turbulent level of the SW-magnetosphere-ionosphere system – a ULF wave power index, derived from ground-based and satellite observations. The wave power index characterizes the ground ULF wave activity on a global scale better than data from selected stations subjected to unavoidable variations of their locations because of Earth's rotation. The new ULF wave power index is a simple and convenient tool for the description of the wave activity in an important and powerful frequency range of the magnetosphere system and it can be applied to various space physics and space weather problems such as:

- SW/IMF interaction with the magnetosphere, in particular, features of the high-speed SW stream interactions,
- discrimination between geoeffective and ineffective high speed streams,
- ring current dynamics,
- search for ULF wave precursors of substorms and storms,
- radiation belt electron acceleration.

Our analysis based on the usage of these indices has elucidated the role of ULF power in the magnetospheric response to SW/IMF forcing. Some of these results are to be understood in the framework of the SW turbulence

theories, such as non-linear growth of IMF fluctuations intensity with the increase of the SW velocity, the occurrence of the saturation level of fluctuations, etc. Similarly, the statistical features of the correspondence between the ground ULF wave intensity and V might be interesting for the theory of ULF wave excitation through the SW shear flow instability. In particular, the observed decrease of the ULF excitation efficiency with the SW V increase contradicts the notion on the over-reflection of magnetospheric ULF modes at the magnetopause under high V (Mann *et al.* 1999).

Using the introduced indices, we have examined statistical relationships between the “killer” electron and ULF activity. As expected, the correlation between the variations of electrons flux and V is high, but at the same time the interconnection between electrons flux and ULF wave power also remains high throughout all phases of solar cycle. This indicates that the mechanism of a “magnetospheric geosynchrotron” contributes (but not as the only one!) to the electron acceleration. Thus, ULF wave index should be included in adequate space radiation models for the prediction of magnetospheric electron flux hazards.

The ULF index database since 1991 up to 2005 is freely available via anonymous FTP server (space.augsburg.edu/MACCS/ULF_index) for all interested researchers for further validation and statistical studies.

Acknowledgments. This study is supported by the grants from INTAS 05-1000008-7978 and YSF 05-109-4661. We appreciate the help of O. Kozyreva in the index production, and useful discussions with N. Crosby and J. Watermann.

References

- Antonova, E.E. (2000), Large scale magnetospheric turbulence and the topology of magnetospheric currents, *Adv. Space Res.* **25**, 7-8, 1567-1570, DOI: 10.1016/S0273-1177(99)00669-9.
- Borovsky, J.E., and H.O. Funsten (2003), Role of solar wind turbulence in the coupling of the solar wind to the Earth’s magnetosphere, *J. Geophys. Res.* **108**, A6, 1246, DOI: 10.1029/2002JA009601.
- Elkington, S.R., M.K. Hudson, and A.A. Chan (1999), Acceleration of relativistic electrons via drift-resonant interaction with toroidal-mode Pc-5 ULF oscillations, *Geophys. Res. Lett.* **26**, 21, 3273-3276, DOI: 10.1029/1999GL003659.
- Engebretson, M., K.-H. Glassmeier, M. Stellmacher, W.J. Hughes, and H. Lühr (1998), The dependence of high-latitude PcS wave power on solar wind velocity and on the phase of high-speed solar wind streams, *J. Geophys. Res.* **103**, A11, 26,271-26,283, DOI: 10.1029/97JA03143.

- Kleimenova, N.G., O.V. Kozyreva, J.J. Schott, J. Bitterly, and P. Ivanova (2003), Dayside geomagnetic Pc5 pulsations in the conditions of a strongly disturbed solar wind during the magnetic storm on 21 February 1994, *Int. J. Geomagnet. Aeron.* **3**, 229-244.
- Kozyreva, O.V., V.A. Pilipenko, M.J. Engebretson, K. Yumoto, J. Watermann, and N. Romanova (2007), In search of a new ULF wave index: Comparison of Pc5 power with dynamics of geostationary relativistic electrons, *Planet. Space Sci.* **55**, 755-769, DOI: 10.1016/j.pss.2006.03.013.
- Mann, I.R., A.N. Wright, K.J. Mills, and V.M. Nakariakov (1999), Excitation of magnetospheric waveguide modes by magnetosheath flows, *J. Geophys. Res.* **104**, A1, 333-353, DOI: 10.1029/1998JA900026.
- Meredith, N.P., M. Cain, R.B. Horne, R.M. Thorne, D. Summers, and R.R. Anderson (2003), Evidence for chorus-driven electron acceleration to relativistic energies from a survey of geomagnetically disturbed periods, *J. Geophys. Res.* **108**, A6, 1248, DOI: 10.1029/2002JA009764.
- O'Brien, T.P., R.L. McPherron, D. Sornette, G.D. Reeves, R. Friedel, and H.J. Singer (2001), Which magnetic storms produce relativistic electrons at geosynchronous orbit? *J. Geophys. Res.* **106**, A8, 15,533-15,544, DOI: 10.1029/2001JA000052.
- Pilipenko, V.A. (1990), ULF waves on the ground and in space, *J. Atmos. Terr. Phys.* **52**, N12, 1193-1209, DOI: 10.1016/0021-9169(90)90087-4.
- Pilipenko, V., N. Yagova, N. Romanova, and J. Allen (2006), Statistical relationships between the satellite anomalies at geostationary orbits and high-energy particles, *Adv. Space Res.* **37**, 1192-1205, DOI: 10.1016/j.asr.2005.03.152.
- Reeves, G.D. (1998), Relativistic electrons and magnetic storms: 1992-1995, *Geophys. Res. Lett.* **25**, 11, 1817-1820, DOI: 10.1029/98GL01398.
- Rostoker, G., S. Skone, and D.N. Baker (1998), On the origin of relativistic electrons in the magnetosphere associated with some geomagnetic storms, *Geophys. Res. Lett.* **25**, 3701-3704, DOI: 10.1029/98GL02801.
- Shevyrev, N.N., and G.N. Zastenker (2005), Some features of the plasma flow in the magnetosheath behind quasi-parallel and quasi-perpendicular bow shocks, *Planet. Space Sci.* **53**, 95-102, DOI: 10.1016/j.pss.2004.09.033.
- Ukhorskiy, A.Y., K. Takahashi, B.J. Anderson, and H. Korth (2005), Impact of toroidal ULF waves on the outer radiation belt electrons, *J. Geophys. Res.* **110**, A10202, DOI: 10.1029/2005JA011017.

Received 3 January 2008

Accepted 17 June 2008